

Cathodoluminescence of rare earth implanted Ga₂O₃ and GeO₂ nanostructures

This article has been downloaded from IOPscience. Please scroll down to see the full text article.

2011 Nanotechnology 22 285706

(<http://iopscience.iop.org/0957-4484/22/28/285706>)

View [the table of contents for this issue](#), or go to the [journal homepage](#) for more

Download details:

IP Address: 140.105.2.12

The article was downloaded on 08/06/2011 at 07:54

Please note that [terms and conditions apply](#).

Cathodoluminescence of rare earth implanted Ga_2O_3 and GeO_2 nanostructures

E Nogales¹, P Hidalgo¹, K Lorenz², B Méndez¹, J Piqueras¹ and E Alves²

¹ Departamento de Física de Materiales, Universidad Complutense, 28040 Madrid, Spain

² Instituto Tecnológico e Nuclear, Estrada Nacional 10, 2686-953 Sacavém, Portugal

E-mail: emilio.nogales@fis.ucm.es

Received 3 March 2011, in final form 5 May 2011

Published 7 June 2011

Online at stacks.iop.org/Nano/22/285706

Abstract

Rare earth (RE) doped gallium oxide and germanium oxide micro- and nanostructures, mostly nanowires, have been obtained and their morphological and optical properties have been characterized. Undoped oxide micro- and nanostructures were grown by a thermal evaporation method and were subsequently doped with gadolinium or europium ions by ion implantation. No significant changes in the morphologies of the nanostructures were observed after ion implantation and thermal annealing. The luminescence emission properties have been studied with cathodoluminescence (CL) in a scanning electron microscope (SEM). Both $\beta\text{-Ga}_2\text{O}_3$ and GeO_2 structures implanted with Eu show the characteristic red luminescence peak centered at around 610 nm, due to the $^5\text{D}_0\text{-}^7\text{F}_2\text{Eu}^{3+}$ intraionic transition. Sharpening of the luminescence peaks after thermal annealing is observed in Eu implanted $\beta\text{-Ga}_2\text{O}_3$, which is assigned to the lattice recovery. Gd^{3+} as-implanted samples do not show rare earth related luminescence. After annealing, optical activation of Gd^{3+} is obtained in both matrices and a sharp ultraviolet peak centered at around 315 nm, associated with the $\text{Gd}^{3+} \text{ } ^6\text{P}_{7/2}\text{-}^8\text{S}_{7/2}$ intraionic transition, is observed. The influence of the Gd ion implantation and the annealing temperature on the gallium oxide broad intrinsic defect band has been analyzed.

1. Introduction

Semiconductor nanowires are emerging as novel building blocks in future nanodevices [1, 2]. In recent years, a large amount of work has been devoted to the control and study of nanostructures of several groups of semiconducting materials, from silicon to oxides. One of the main goals is to exploit the high potential of semiconductor nanowires. One way is the control of doping processes leading to feasible electronic and optoelectronic devices [3, 4]. Semiconductor nanowires are difficult to dope by diffusion methods because they usually exhibit very high crystal quality, which leaves no place for foreign atoms, and also due to impurity out-diffusion processes during growth [5, 6]. Ion implantation is routinely used to dope thin layers of semiconductors with a high control of the dopant concentration and penetration depth with the objective of achieving p- or n-type doping or of modifying their luminescence properties [7, 8]. However, this approach

has not yet been much explored in semiconductor nanowires and only a few works related to doping by ion implantation of nanowires have been published, e.g. [3, 6, 9]. In these works, doping was focused toward electronic functionality of silicon nanowires. However, other outstanding and emergent applications of semiconductor nanostructures are their tunable luminescence properties as a function of doping [4, 10, 11]. In particular, rare earth (RE) ions, such as Er^{3+} , have been widely investigated in silicon nanocrystals [12, 13], but the study of luminescence from RE ions hosted in nanowires is still under research [4, 11, 14].

Both GeO_2 and $\beta\text{-Ga}_2\text{O}_3$ belong to the family of the transparent conductive oxides (TCO). They have band gaps of almost 5 eV and are therefore transparent in the infrared (IR), visible and ultraviolet (UV), down to about 260 nm. There is a strong interest in these materials for optoelectronic applications in the UV-visible range. Gadolinium and europium present efficient luminescence lines in the ultraviolet

and red ranges, respectively. While the Eu^{3+} luminescence has been quite extensively studied in different hosts, including nanostructures [7, 11, 14, 15], Gd^{3+} has only been studied in bulk wide band gap materials [16–21].

In this work, we have doped semiconductor oxide (GeO_2 and $\beta\text{-Ga}_2\text{O}_3$) micro- and nanostructures with rare earth ions (Eu^{3+} , Gd^{3+}) by ion implantation in order to get efficient UV and visible light emission, even at room temperature. The luminescence properties have been studied by cathodoluminescence (CL) in a scanning electron microscope (SEM), which enabled us to discuss the obtained results in the light of the relationship between intrinsic defects and the recovery of crystal quality after the implantation damage.

2. Experimental details

Undoped gallium oxide nanostructures have been obtained by a vapor–solid growth mechanism from metallic gallium in a tube furnace, as explained elsewhere [14]. The substrate was a gallium oxide pellet and no catalyst was used. GeO_2 nanostructures were grown from Ge powder with 99.999% purity as starting material by thermal treatment at 600°C under argon flow for 6 h. After the growth process, some of the structures were placed on silicon or graphite substrates. Ion implantation was performed with either europium or gadolinium ions with an energy of 150 or 300 keV and fluences in the range 10^{14} – 10^{16} cm^{-2} . In order to obtain crystal recovery after implantation, thermal annealing of the implanted samples was performed at temperatures in the range 500 – 1100°C for $\beta\text{-Ga}_2\text{O}_3$ and in the range 100 – 500°C for GeO_2 . A Leica Stereoscan 440 SEM was used for morphological characterization. Rutherford backscattering spectroscopy (RBS) measurements were performed with a 1 mm diameter collimated beam of 2 MeV He^+ ions. The backscattered particles were detected at a scattering angle of 140° , using a silicon surface barrier detector with a resolution of 13 keV. CL measurements were performed within the above mentioned Leica system or in a Hitachi S2500 SEM. CL spectra were recorded with a Hamamatsu PMA-11 charge coupling device camera.

3. Results and discussion

Figure 1 shows representative SEM images of RE implanted and subsequently annealed micro- and nanostructures of GeO_2 and Ga_2O_3 . Figure 1(a) shows GeO_2 nano- and microwires implanted with Eu with a fluence of 10^{16} cm^{-2} at 300 keV and annealed at 500°C on graphite. The widths of the structures range from a few hundred nanometers to a few microns and the lengths up to several tens of microns. Figure 1(b) shows $\beta\text{-Ga}_2\text{O}_3$ nanowires implanted with Gd with a fluence of $5 \times 10^{15}\text{ cm}^{-2}$ at 150 keV and annealed at 700°C . In this case, the lateral dimensions range from some tens to a few hundred nanometers and the lengths can be up to a few tens of microns. The morphologies of the structures have not been affected by ion implantation and subsequent thermal annealing, as can be observed from comparison with undoped GeO_2 ([22],

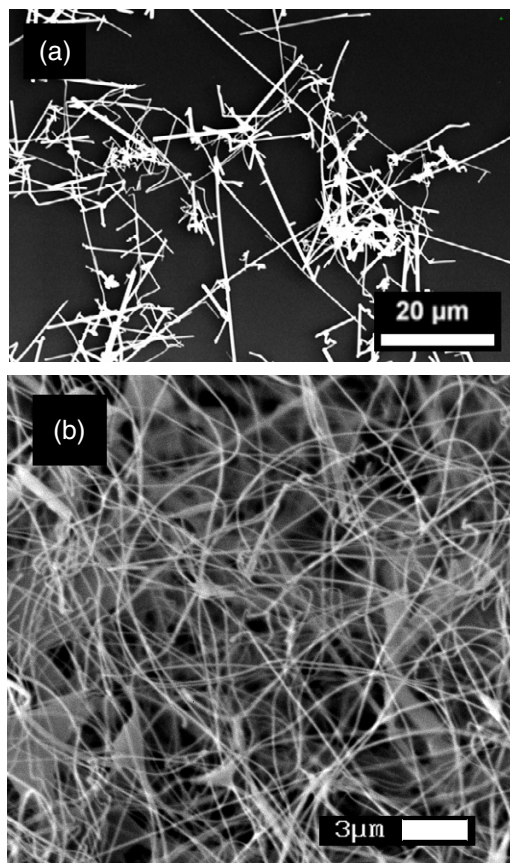


Figure 1. SEM images of (a) Eu implanted and annealed GeO_2 nanowires on graphite and (b) Gd implanted and annealed $\beta\text{-Ga}_2\text{O}_3$ nanowires.

figure 2) and Ga_2O_3 ([14], figure 2) nanowires obtained in the same conditions.

Figure 2 shows RBS spectra from the GeO_2 (figure 2(a)) and $\beta\text{-Ga}_2\text{O}_3$ (figure 2(b)) structures on graphite before and after implantation of Eu with a 10^{16} cm^{-2} fluence and a 300 keV energy. A clear signal related to the Eu can be observed in the implanted samples. However, implantation was performed at the same time in the structures and the graphite substrate, so that the rare earth signal comes from the ions in both hosts and further analysis on the penetration depth of europium in the nanostructures cannot be performed. RBS spectra from the Gd implanted samples (not shown) present a similar behavior, with a clear signal related to the rare earth.

Figures 3(a) and (b) show the CL spectra acquired at 100 K and RT, respectively, from europium implanted GeO_2 structures with a fluence of 10^{16} cm^{-2} and energy of 300 keV after annealing at 500°C . A sharp peak centered at around 610 nm, related to the $^5\text{D}_0\text{--}^7\text{F}_2$ Eu^{3+} intraionic transition, is clearly observed at room temperature, while it is very weakly observed at low temperature, because of the very intense intrinsic defect related band. On the other hand, figure 3(c) shows the CL spectrum before annealing, in which the Eu^{3+} luminescence peak is also observed. It is worth mentioning that the Eu^{3+} luminescence in implanted GeO_2 nanostructures is much more intense than the luminescence due to Eu incorporation by thermal diffusion in GeO_2 nanowires [11]. In

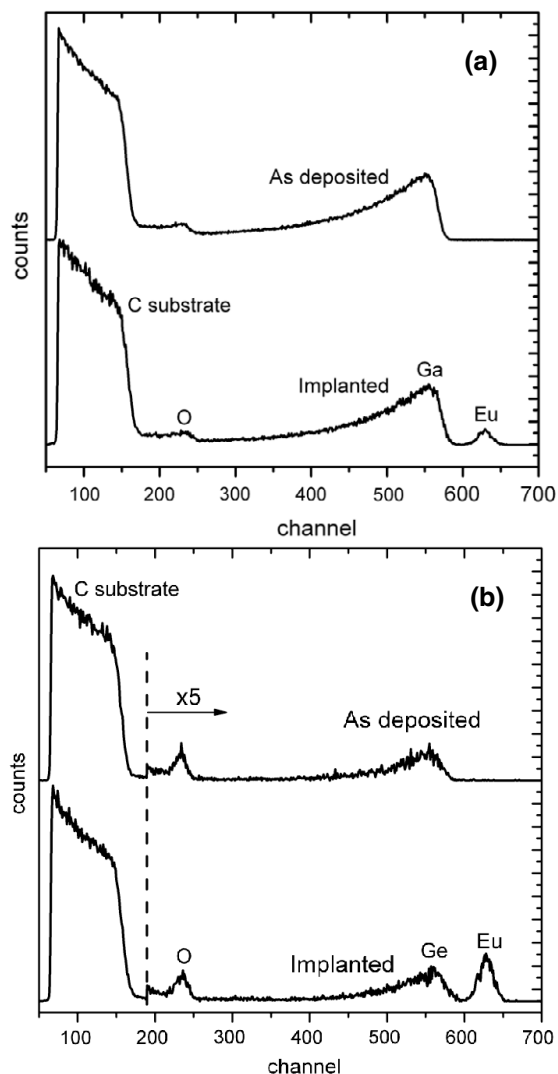


Figure 2. RBS spectra from as-deposited and implanted (a) β -Ga₂O₃ and (b) GeO₂ micro- and nanostructures on graphite.

the previous work [11], Eu emission was scarcely detected at room temperature in the slope of the broad defect band, while a narrow line is clearly observed in the current Eu implanted samples.

Figure 4(a) shows the normalized CL spectra from Eu implanted ($5 \times 10^{15} \text{ cm}^{-2}$, 150 keV) β -Ga₂O₃ microstructures. The spectra are acquired before (top spectrum) and after (bottom) annealing at 1100 °C. As in the case of GeO₂, efficient red luminescence emission is observed even before the thermal treatment. In the case of Ga₂O₃ matrix, as-implanted samples show wider peaks related to the $^5\text{D}_0$ – $^7\text{F}_j$ Eu³⁺ intraionic transitions than in annealed samples. Moreover, the peak maximum, around 610 nm, is slightly shifted to longer wavelengths in as-implanted samples.

We have performed, for comparison, similar measurements in a polycrystalline pellet that was implanted with Eu and annealed under the same conditions as the structures. The spectra from the as-implanted (top spectrum) and implanted and annealed (bottom) pellet are shown in figure 4(b). The peaks observed in the two spectra have the same shapes as

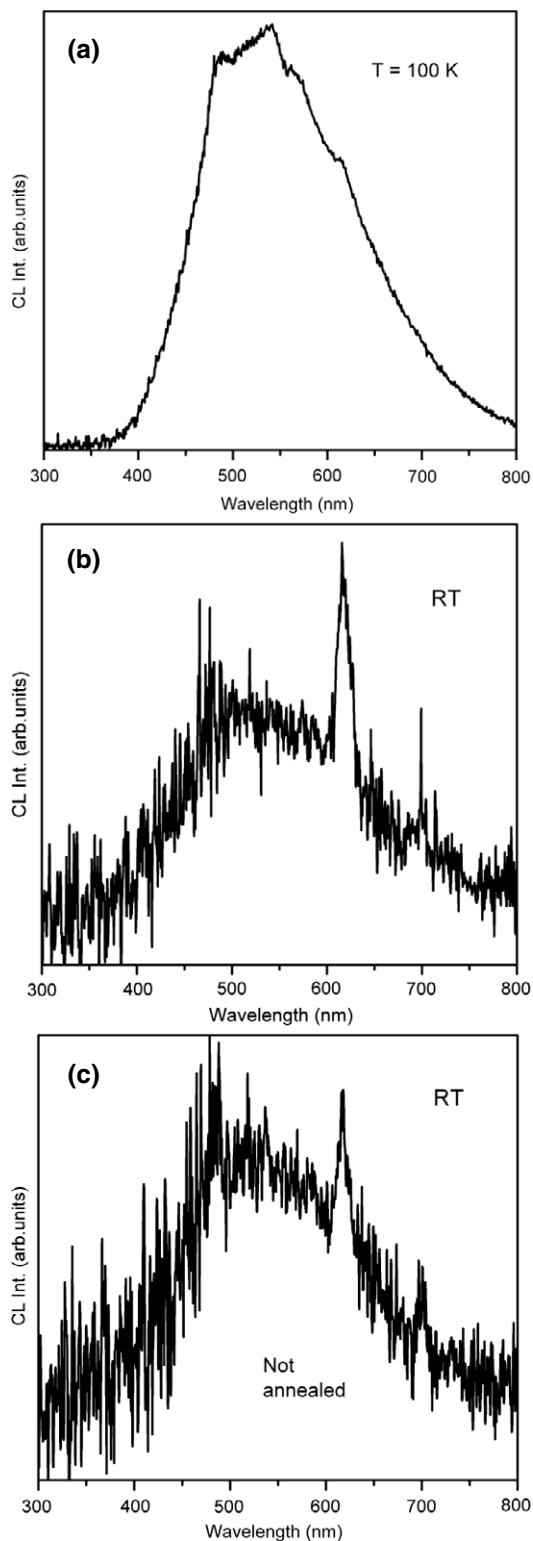


Figure 3. CL spectra acquired at (a) $T = 100 \text{ K}$ and (b) RT from GeO₂ nanowires implanted with europium at a fluence of 10^{16} cm^{-2} , energy of 300 keV and annealed at 500 °C. The $^5\text{D}_0$ – $^7\text{F}_2$ Eu³⁺ intraionic transition is clearly observed at room temperature. (c) CL spectrum from the as-implanted nanowires.

those shown in figure 4(a), indicating that the emission centers are the same in the microstructures and in the polycrystalline pellet and that the annealing has a similar effect on the

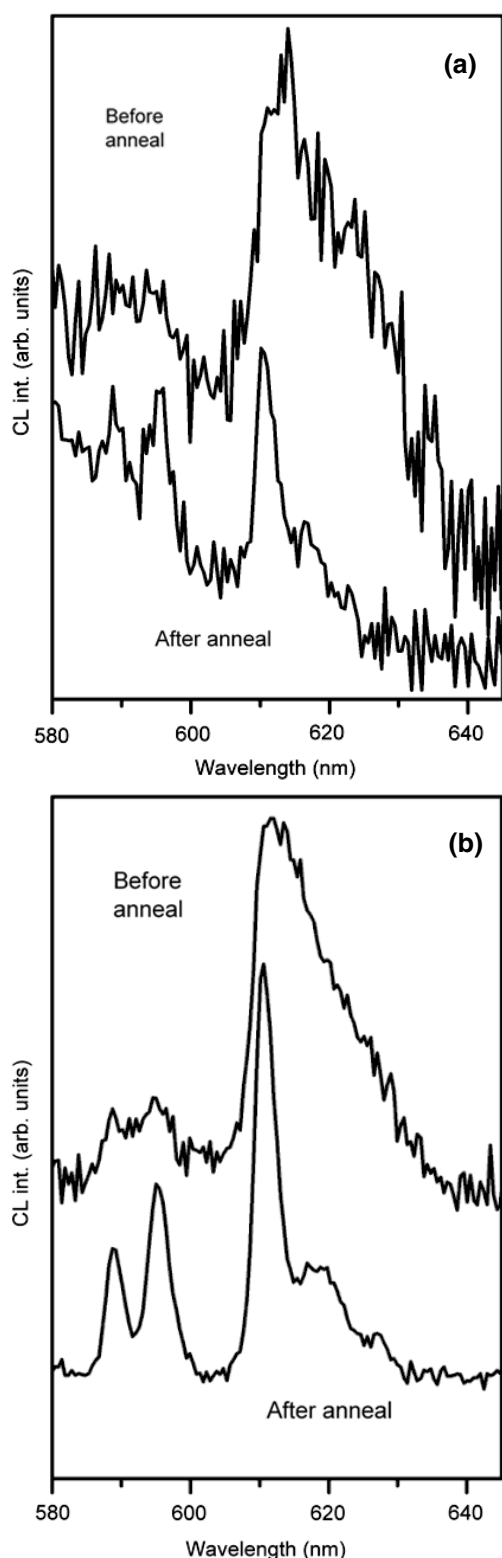


Figure 4. Normalized room temperature CL spectra from Eu implanted ($5 \times 10^{15} \text{ cm}^{-2}$, 150 keV) $\beta\text{-Ga}_2\text{O}_3$ (a) microstructures and (b) polycrystalline pellet, before (top) and after (bottom) thermal annealing at $T_{\text{ann}} = 1100^\circ\text{C}$.

luminescence. In a previous work where $\beta\text{-Ga}_2\text{O}_3$ nanowires were doped with europium through a diffusion process, a discussion of the luminescence of several Eu^{3+} centers, in

Eu_2O_3 , $\text{Eu}_3\text{Ga}_5\text{O}_{12}$ or $\beta\text{-Ga}_2\text{O}_3$, was carried out and a peak at 610 nm was assigned to Eu^{3+} in the $\beta\text{-Ga}_2\text{O}_3$ host [14]. This supports the idea that the peaks observed after annealing in the present work correspond to this luminescence center and that no other phases or aggregates were formed during the implantation and annealing processes. XRD measurements (not shown) have been performed and the observed peaks were associated with either gallium oxide (JCPDS 00-041-1103) or the silicon substrate. No peaks related to complexes that include Eu were found, further supporting the idea that the luminescence peaks correspond to Eu^{3+} within the monoclinic gallium oxide host.

The broadening of the peaks before annealing can be explained as follows. The positions of the rare earth 4f electronic energy levels, responsible for the luminescence peaks, are almost independent of the local crystal field due to the screening by the filled $5s^25p^6$ outer electron shells [23]. However, in spite of this screening, a weak interaction is still present and slight energy shifts of the peaks occur when the local crystal field is modified due to the presence of defects. In our case, the severe damage created by the ion implantation creates an inhomogeneous environment for the ions. Therefore, the broadening of the rare earth luminescence peaks before annealing is explained by the implantation damage. After annealing, sharpening of the lines is due to the lattice recovery that results in almost identical site symmetry for most of the Eu^{3+} ions. A consequence of this result is that the Eu^{3+} luminescence peaks can be used as a probe to monitor the recovery of the lattice disorder in nanowires during post-implant annealing.

The high interest in ultraviolet emission devices motivates the study of Gd implantation in semiconductor oxide nanostructures. Its characteristic intraionic transition ${}^6\text{P}_{7/2} - {}^8\text{S}_{7/2}$ at 3.96 eV lies beyond the band gap of common semiconductor oxides, such as ZnO. For this reason, GeO_2 and $\beta\text{-Ga}_2\text{O}_3$ are expected to be suitable hosts in order to get UV luminescence from the Gd ions. Figure 5 shows the CL spectra of Gd implanted GeO_2 acquired at $T = 100 \text{ K}$ (figure 5(a)) and at room temperature (figure 5 (b)). The characteristic $\text{Gd}^{3+} {}^6\text{P}_{7/2} - {}^8\text{S}_{7/2}$ intraionic transition is observed only at low temperature (see the inset in figure 5(a)), but cannot be observed at room temperature. It should be noticed that for Eu implanted GeO_2 (see figure 3), the $\text{Eu}^{3+} {}^5\text{D}_0 - {}^7\text{F}_2$ luminescence peak was observed at room temperature, but scarcely at $T = 100 \text{ K}$, because of the defect band in the same energy range. Gd emission at low temperature is clearly identified, but its efficiency in GeO_2 is not high enough to be measured at room temperature. These results suggest a different interaction process between the electronic levels involved in the excitation and de-excitation of the two rare earth ions within the GeO_2 matrix.

Figure 6 (top spectrum) shows the CL spectrum from the $\beta\text{-Ga}_2\text{O}_3$ nanowires shown in figure 1(b), implanted with Gd at a fluence of $5 \times 10^{15} \text{ cm}^{-2}$ and energy of 150 keV and annealed at 700°C . They present an intense peak centered at 313 nm, due to the $\text{Gd}^{3+} {}^6\text{P}_{7/2} - {}^8\text{S}_{7/2}$ intraionic transition, thus confirming the efficient emission of the implanted gadolinium within the $\beta\text{-Ga}_2\text{O}_3$ nanowires. For comparison, the CL

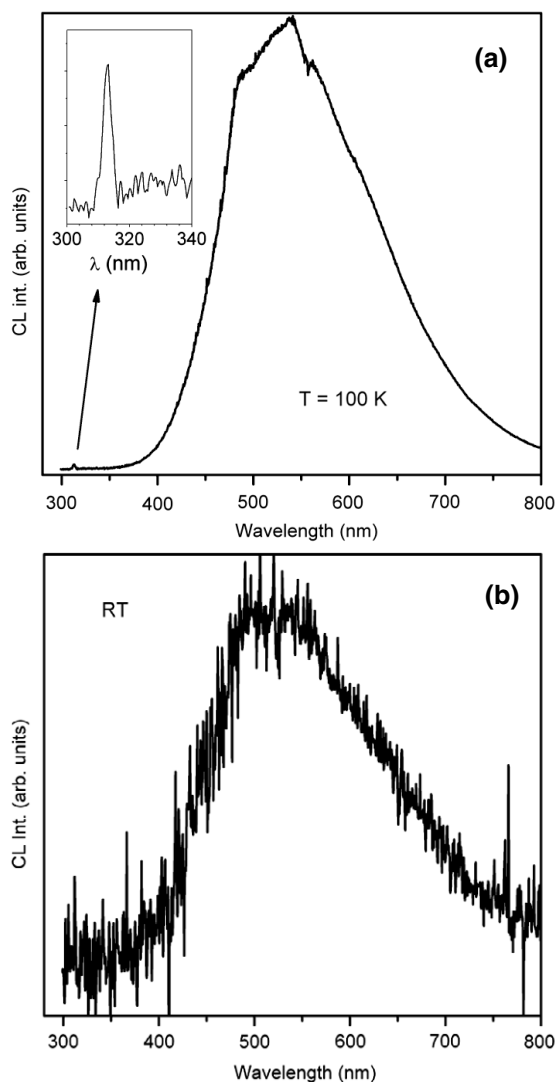


Figure 5. CL spectra from Gd implanted GeO_2 nanostructures at (a) $T = 100$ K and (b) room temperature.

spectrum from undoped nanowires is also shown in figure 6 (bottom spectrum). The emission observed in the undoped nanowires is the characteristic $\beta\text{-Ga}_2\text{O}_3$ band associated with oxygen vacancies [24, 25]. This intrinsic defect band is also observed in the Gd implanted nanowires, but it appears broader and with additional components at longer wavelengths.

Although significant Gd^{3+} related luminescence in $\beta\text{-Ga}_2\text{O}_3$ nanostructures was observed at room temperature, the CL intensity was not very high. Hence, in order to further discuss the influence of the implantation on the luminescence of the $\beta\text{-Ga}_2\text{O}_3$ nanowires observed in figure 6, a CL study from Gd implanted and annealed polycrystalline pellets has also been performed. Figure 7(a) presents the CL spectra acquired at different acceleration voltages (V_{acc}) from a Gd implanted $\beta\text{-Ga}_2\text{O}_3$ pellet in the same conditions as the nanowires shown above, but annealed at 500°C . It is clearly observed that at low voltages, $V_{\text{acc}} = 2\text{--}3$ kV, the Gd^{3+} related 313 nm luminescence peak completely dominates the spectrum and the $\beta\text{-Ga}_2\text{O}_3$ intrinsic defect band is hardly observed. On the other hand, at a higher voltage, $V_{\text{acc}} = 5$ kV, the defect

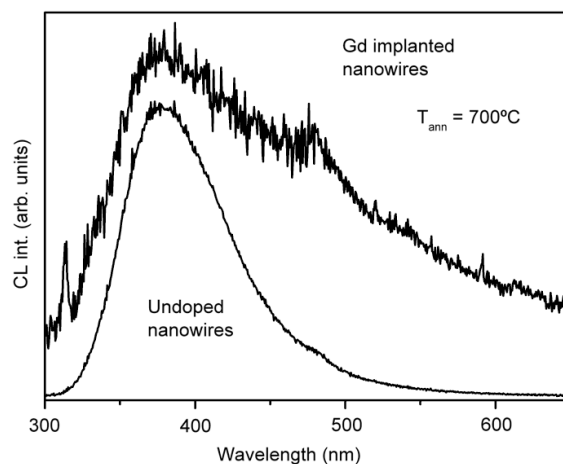


Figure 6. Room temperature CL spectra acquired at $V_{\text{acc}} = 5$ kV from undoped nanowires (bottom spectrum) and Gd implanted nanowires annealed at 700°C (top spectrum).

band acquires an intensity similar to that of the Gd^{3+} peak. These results can be explained by the dependence of CL signal generation volume on the acceleration beam voltage.

Simulations for the penetration profiles of the implanted ions and the accelerated electrons have been performed with TRIM [5] and CASINO [26] software, respectively, both based on Monte Carlo calculations. Figure 7(b) shows the depth profiles obtained from these simulations. The profile of the Gd ions implanted in $\beta\text{-Ga}_2\text{O}_3$ with an energy of 150 keV (bottom) shows that the maximum concentration is obtained at a depth of around 30 nm and the maximum penetration depth is around 70 nm. On the other hand, the penetration profiles of the electrons for $V_{\text{acc}} = 2, 3$ and 5 kV are represented in the same depth range (top). Comparison of the TRIM and CASINO profiles shows that for $V_{\text{acc}} = 2$ and 3 kV the electrons stop within the implanted and damaged volume of the gallium oxide. However, for $V_{\text{acc}} = 5$ kV a considerable fraction of the incident electrons penetrate deep enough into the material, exciting the luminescence in undamaged material as well. Therefore, agreement between the simulations in figure 7(b) and the CL experimental results in figure 7(a) is obtained.

Finally, it is well known that the lattice recovery and optical activation of implanted optically active ions strongly depends on the annealing temperature [27]. Hence, we have studied the influence of the annealing temperature on the CL spectra of Gd implanted $\beta\text{-Ga}_2\text{O}_3$ samples. CL spectra from samples annealed at $500, 700$ and 1100°C acquired at 2 kV with low excitation density conditions are shown in figure 7(c). Two relevant facts can be deduced from the CL spectra. Firstly, the Gd^{3+} line intensity is the only emission for low annealing temperature (500°C) and a complete quenching of the native defects band is observed. It should be noticed that no CL emission was observed in the as-implanted samples, hence the low temperature annealing activates the RE emission. Secondly, a higher relative intensity of the $\beta\text{-Ga}_2\text{O}_3$ defect band with respect to the Gd^{3+} peak is obtained when the annealing temperature is increased. In

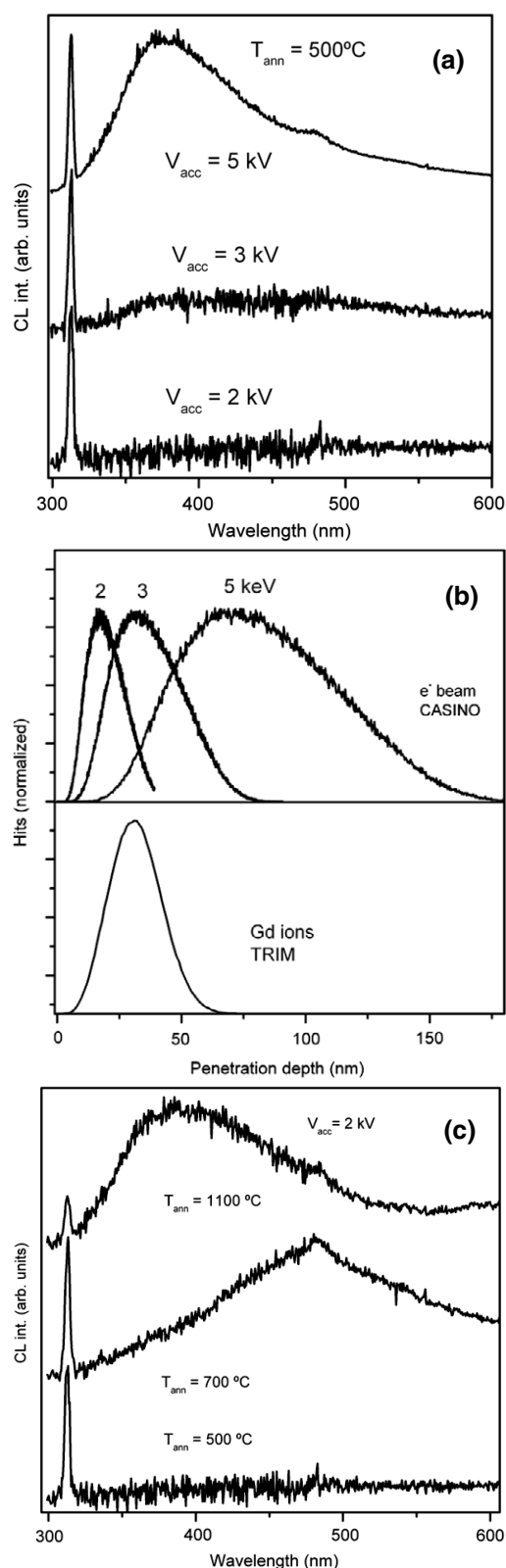


Figure 7. (a) Normalized room temperature CL spectra from a Gd implanted gallium oxide pellet annealed at 500 °C at three different acceleration voltages. (b) TRIM simulation (bottom) for the penetration depth of the Gd implanted ions. CASINO simulation (top) for the penetration depth of the electron beam at $V_{acc} = 5$ kV, $V_{acc} = 3$ kV and $V_{acc} = 2$ kV. (c) Normalized CL spectra acquired at $V_{acc} = 2$ keV and low excitation density conditions from Gd implanted gallium oxide pellets annealed at the three temperatures 500, 700 and 1100 °C.

addition, the shape of the CL defect band changes with the annealing temperature. In particular, the defect band obtained for the sample annealed at 700 °C is shifted toward lower energies and does not correspond to the characteristic intrinsic β -Ga₂O₃ defect band. This emission is rather related to the complex, longer wavelength bands of Gd implanted and 700 °C annealed nanowires, shown in figure 6. At $T_{ann} = 1100$ °C, at which a higher lattice recovery takes place, the CL spectrum is dominated by the characteristic gallium oxide intrinsic defect band. Therefore, the lack of the gallium oxide native defects band at low annealing temperatures can be interpreted as quenching of the radiative transitions of the native intrinsic defects due to the implantation induced defects, which are not removed at such low annealing temperatures. The shifted broad band observed in both the nanowires and the polycrystalline pellet that were annealed at 700 °C can therefore be associated with the defects created during implantation that are still present after the partial lattice recovery.

4. Summary

Summarizing, we have demonstrated effective rare earth doping of β -Ga₂O₃ and GeO₂ micro- and nanostructures by ion implantation. The characteristic red Eu³⁺ emission lines have been observed in both host materials even at room temperature. Ultraviolet Gd³⁺ emission was also observed at room temperature in β -Ga₂O₃ nanowires, while it could only be seen at low temperatures for the case of GeO₂ nanowires. A strong influence of the annealing treatments on the luminescence spectra after ion implantation is observed. Eu³⁺ luminescence lines are observed in as-implanted samples, but sharpening of the peaks is observed after annealing implanted gallium oxide structures, which is attributed to the lattice recovery. After annealing, the Gd³⁺ UV related line is observed in GeO₂ at low temperatures and in β -Ga₂O₃ up to room temperature. Optical activation of the rare earth is obtained at 500 °C in both materials. For annealing at this low temperature the gallium oxide intrinsic defect band is quenched. After annealing at 1100 °C the intrinsic defect band is recovered.

Acknowledgments

This work has been supported by MICINN (Projects MAT 2009-07882 and Consolider Ingenio CSD 2009-00013). The authors also thank the bilateral Spanish–Portuguese project HP-2008-0071 and FCT Portugal (Ciência 2007 and PTDC/CTM/100756/2008).

References

- [1] Barth S, Hernandez-Ramirez F, Holmes J D and Romano-Rodriguez A 2010 *Prog. Mater. Sci.* **55** 563
- [2] Law M, Sirbuly D J, Johnson J C, Goldberger J, Saykally R J and Yang P 2004 *Science* **305** 1269
- [3] Colli A, Fasoli A, Ronning C, Pisana S, Piscanec S and Ferrari A C 2008 *Nano Lett.* **8** 2188

- [4] Nogales E, Garcia J A, Mendez B and Piqueras J 2007 *Appl. Phys. Lett.* **91** 133108
- [5] Borschel C, Niepelt R, Geburt S, Gutsche C, Regolin I, Prost W, Tegude F J, Stichtenoth D, Schwen D and Ronning C 2009 *Small* **5** 2576
- [6] Ronning C, Borschel C, Geburt S and Niepelt R 2010 *Mater. Sci. Eng. R* **70** 30
- [7] Wang K, Martin R W, Nogales E, Edwards P R, O'Donnell K P, Lorenz K, Alves E and Watson I M 2006 *Appl. Phys. Lett.* **89** 131912
- [8] Nogales E, García J A, Méndez B, Piqueras J, Lorenz K and Alves E 2008 *J. Phys. D: Appl. Phys.* **41** 065406
- [9] Hoffmann S, Bauer J, Ronning C, Stelzner Th, Michler J, Ballif C, Sivakov V and Christiansen S H 2009 *Nano Lett.* **9** 1341
- [10] Müller S, Zhou M, Li Q and Ronning C 2009 *Nanotechnology* **20** 135704
- [11] Hidalgo P, Liberti E, Rodriguez-Lazcano Y, Mendez B and Piqueras J 2009 *J. Phys. Chem. C* **113** 17200
- [12] Franzò G, Pacifici D, Vinciguerra V, Priolo F and Iacona F 2000 *Appl. Phys. Lett.* **76** 2167
- [13] Kik P G, Brongersma M L and Polman A 2000 *Appl. Phys. Lett.* **76** 2325
- [14] Nogales E, Mendez B, Piqueras J and Garcia J A 2009 *Nanotechnology* **20** 115201
- [15] Wang K, Martin R W, O'Donnell K P, Katchkanov V, Nogales E, Lorenz K, Alves E, Ruffenach S and Briot O 2005 *Appl. Phys. Lett.* **87** 112107
- [16] Toyama T, Ota J, Adachi D, Niioka Y, Lee D H and Okamoto H 2009 *J. Appl. Phys.* **105** 084512
- [17] Zavada J M *et al* 2006 *Appl. Phys. Lett.* **89** 152107
- [18] Vetter U, Zenneck J and Hofsäss H 2003 *Appl. Phys. Lett.* **83** 2145
- [19] Gruber J B, Vetter U, Hofsäss H, Zandi B and Reid M F 2004 *Phys. Rev. B* **69** 195202
- [20] Prucnal S, Sun J M, Rebohle L and Skorupa W 2007 *Appl. Phys. Lett.* **91** 181107
- [21] Sun J M, Prucnal S, Skorupa W, Dekorsy T, Mücklich A and Helm M 2006 *J. Appl. Phys.* **99** 103102
- [22] Hidalgo P, Méndez B and Piqueras J 2008 *Nanotechnology* **19** 455705
- [23] Przybylinska H, Jantsch W, Suprun-Belevitch Yu, Stepikhova M, Palmetshofer L, Hendorfer G, Kozanecki A, Wilson R J and Sealy B J 1996 *Phys. Rev. B* **54** 2532
- [24] Binet L and Gourier D 1998 *J. Phys. Chem. Solids* **59** 1241
- [25] Nogales E, Mendez B and Piqueras J 2005 *Appl. Phys. Lett.* **86** 113112
- [26] Drouin D, Couture A R, Joly D, Tastet X, Aimez V and Gauvin R 2007 *Scanning* **29** 92
- [27] Lorenz K, Wahl U, Alves E, Dalmasso S, Martin R W, O'Donnell K P, Ruffenach S and Briot O 2004 *Appl. Phys. Lett.* **85** 2712